

The exclusive license for this PDF is limited to personal printing only. No part of this digital document may be reproduced, stored in a retrieval system or transmitted commercially in any form or by any means. The publisher has taken reasonable care in the preparation of this digital document, but makes no expressed or implied warranty of any kind and assumes no responsibility for any errors or omissions. No liability is assumed for incidental or consequential damages in connection with or arising out of information contained herein. This digital document is sold with the clear understanding that the publisher is not engaged in rendering legal, medical or any other professional services.

### *Chapter 3*

## **CHARACTERIZATION AND APPLICATIONS OF INDUSTRIAL WASTES WITH HIGH CONTENT OF GYPSUM**

*M. J. Gázquez<sup>a\*</sup>, J. P. Bolívar<sup>a</sup>, J. Mantero<sup>b</sup>,  
R. García-Tenorio<sup>b</sup> and F. Vaca<sup>a</sup>*

<sup>a</sup> Department of Applied Physics, University of Huelva, Huelva, Spain

<sup>b</sup> Department of Applied Physics II, University of Seville, Spain

### **ABSTRACT**

The recycling of inorganic wastes generated by different industrial processes is a research field of high interest because the minimization of waste disposal, avoiding its potential release into the environment, can generate environmental and economical benefits for these industries and the general population. The appropriate treatment of industrial wastes could even lead to the generation of co-products of economic value and broad application. Obviously, the environmental and health impact of these co-products should comply with existing regulations.

In this direction, the present study describes first the used raw materials ilmenite (ILM) and slag (SLAG) and a waste known as “red gypsum” (RG) coming from a titanium dioxide industrial facility located at the province of Huelva (Spain), in terms of their elemental composition, radioactive contents, granulometry, mineralogy, microscopic morphology and physical composition. The main goal was to obtain basic information for future potential applications of the RG waste in construction, civil engineering, etc. One of these applications has been studied in the second part of our study: we have analysed the main properties of cements produced with different proportions of red gypsum, and their obtained improvements, in relation to Ordinary Portland Cements (OPC). In the produced RG cements, it has been also demonstrated that the levels of pollutants associated always remain within safety limits.

---

\* Corresponding author: manuel.gazquez@dfa.uhu.es; bolivar@uhu.es; manter@us.es gtenorio@us.es; galan@uhu.es.

## 1. INTRODUCTION

The recycling of waste material generated in the majority of industrial production processes is in the last years the subject of more and more research for several reasons. The protection of health and the environment are of great importance, although the economic benefits accruing from waste recycling cannot be neglected either [1-4]. The minimisation of waste disposal, and/or the minimisation of its direct release into the environment, generates not only health and environmental benefits: in several industrial processes, in addition to the generation of the main product, the appropriate treatment of a fraction of the waste generated could lead to the production of co-products with economic value and broad applications [5-7].

One well known potential use of some industrial wastes is through their incorporation in the cement industry [8-11]. The recycling of waste in the cement industry is performed in two ways: the waste is either a component of the clinker generated as a basis of the cement, or the waste is added to the previously generated clinker to make commercial cement.

There is a paradigmatic NORM (Naturally Occurring Radioactive Material) industry, in south-western Spain, which produces titanium dioxide pigments by applying the so-called sulphate method. In the production process the red gypsum (mostly calcium sulphate) waste is generated which, until now, has not had any use and has been disposed of in an authorized area. This policy has been costly, so the company decided to re-evaluate its options on this waste.

In this industry, the two main raw materials used as feedstock are ilmenite ( $\text{FeTiO}_3$ ) and titaniferous slag. Ilmenite is a heavy mineral containing approximately 43% to 65% titanium dioxide [12], while titaniferous slag, which contains 70% to 80% titanium dioxide, is a co-product of smelting the ilmenite in order to decrease the reagent consumption and waste material accumulation in the subsequent pigment-making process [13]. Slag is used to remove (or at least to reduce) the iron input in the titanium dioxide chemical process, thus obtaining a high titania-slag and marketable iron metal [13,14]. Ilmenite smelting is a carbothermic process that upgrades the ilmenite concentrate, yielding a  $\text{TiO}_2$ -rich slag as primary product and pig iron as co-product [15,16]. In this process, the separation of titanium from iron is based on the considerable difference between titania-slag and metallic iron densities [17].

In the Huelva factory, the oldest and most common process for titanium dioxide production is used: the sulphate process. This process uses concentrated sulphuric acid ( $\text{H}_2\text{SO}_4$ ) to dissolve the titaniferous feedstocks which are milled and dried beforehand to aid the digestion process.

The main steps in the  $\text{TiO}_2$  production process at the Huelva factory, shown in figure 1, are the following:

1. *Digestion of the ore (batch operation)*. A carefully controlled blend of ilmenite and slag is mixed with highly-concentrated sulphuric acid (80%-95%) to digest the  $\text{TiO}_2$ -containing feedstock. A highly-exothermic reaction is initiated by the addition of defined amounts of steam, water and diluted acid.

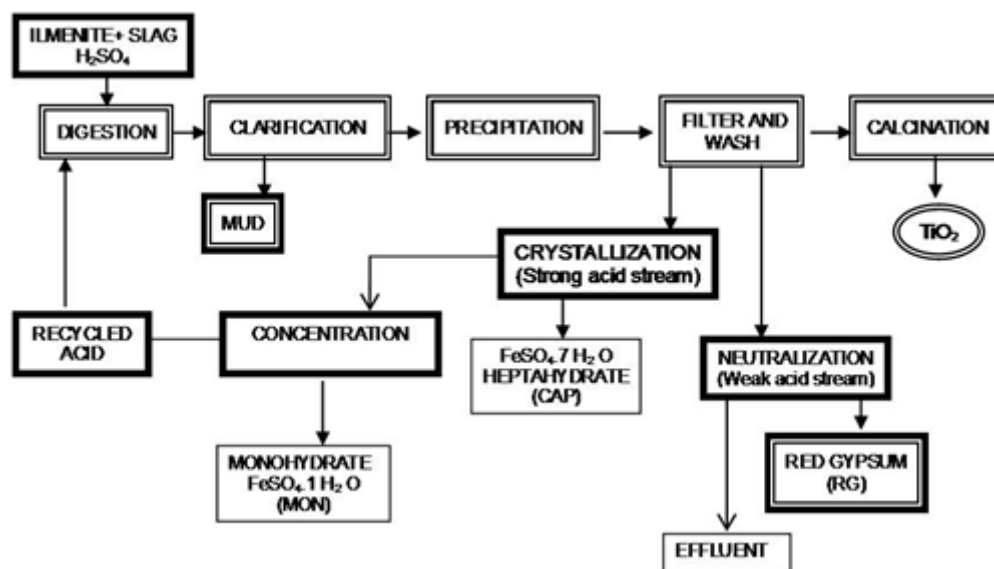
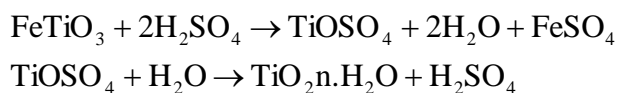


Figure 1. Diagram of the sulphate process used in the Huelva factory

The digestion reaction process can be summarized as:



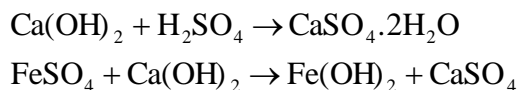
The resulting liquor contains titanyl sulphate ( $\text{TiOSO}_4$ ) and iron sulphate ( $\text{FeSO}_4$ ) dissolved in sulphuric acid. To ensure that all the Fe is in dissolution, the liquor is passed through scrap metal (Fe reduction step)

2. *Clarification of the resulting liquor.* The reduced liquor passes to a clarification tank where the undissolved solids (mud) are allowed to settle; afterwards, the mud is separated from the solution by flocculation (decantation) and filtration. Nowadays, this mud is neutralised and, finally, disposed of in a controlled disposal area.
3. *Titanium dioxide precipitation.* Hydrated titanium dioxide is produced by hydrolysing the clarified liquor with steam. Precipitation of the hydrated  $\text{TiO}_2$  is achieved by boiling the liquor for several hours followed by cooling. The addition of a correct amount of titanium-containing seed nuclei to the batch determines the final size and form of the titanium dioxide crystal.
4. *Hydrated  $\text{TiO}_2$  separation.* The precipitated hydrated  $\text{TiO}_2$  is separated by vacuum filters (called “Moore filters”) from the mother liquor (commonly referred to as “strong” acid, 20%-25%  $\text{H}_2\text{SO}_4$ ). This mother liquor is not considered as a waste of the process, being treated for the generation of two co-products with established markets, as will be detailed later.

5. *TiO<sub>2</sub> washing*. After the separation of the mother liquor, the filtered TiO<sub>2</sub> cake is washed with water or with a weak acid solution in order to remove the remaining impurities. The water or weak acid solution used in this final wash is considered an effluent of the process, which is treated for the generation of a third co-product, as is detailed in the following paragraphs.
6. The washed TiO<sub>2</sub> pulp is then placed in rotary kilns for the removal of its water content and some traces of sulphur. The resulting solid is cooled, milled, coated, washed, dried and finely ground (“micronized”), before be packed for commercial distribution.

The mother liquor effluent (“strong” acid, 20%-25% H<sub>2</sub>SO<sub>4</sub>) resulting from separation of the precipitated TiO<sub>2</sub>, is initially pumped to batch cooler crystallisers, where the bulk of the iron sulphate is removed as solid ferrous sulphate heptahydrate. This constitutes the first co-product of the TiO<sub>2</sub> process, commonly known as cooperas (CAP). The remaining strong acid is then concentrated for reuse in the initial digestion step. This concentration is achieved by multi-stage evaporation up to concentrate the acid, with the remaining ferrous sulphate in the concentrated acid solution being present in the monohydrate rather than the heptahydrate form at the high temperatures employed. This ferrous sulphate monohydrate (MON) precipitates in the concentration step, forming a solid co-product which is separated by filtration.

On the other hand, the second effluent formed by the solution resulting from the final stages of washing TiO<sub>2</sub>, is also processed by sending it to a neutralization plant. The neutralisation step is based on the addition of lime, or limestone, to the weak acid stream, generating a co-product called red gypsum (RG), formed mainly by gypsum and iron hydroxides, according to the following reactions:



The red gypsum is separated by filtration, and the resulting clean water is partially recycled in the process while the remaining one is released into the estuary where the factory is located. The concentrations of pollutants in these waters are substantially lower than the limits fixed by the Spanish government for environmental emissions, not causing their release to the estuary an environmental impact.

The magnitude of the co-products generated at the Huelva factory is reflected clearly in the following figures: Annually, around 142000 metric tonnes of raw material are processed (80 % ilmenite and 20 % slag), with the generation of 70,000 metric tonnes of RG, 140,000 metric tonnes of CAP and 125,000 metric tonnes of MON. The CAP has a defined market for treatment of basic soils in agriculture, as a component in animal feeding or as a flocculants in water treatment, while the iron sulphate monohydrate is used as a raw material in the production of ferric fertilizers for their use in agricultural soils with deficiency of iron.

The use in cement production of waste generated in several industrial activities should be undertaken with caution. Certain requirements should be met: a) the physical and chemical properties of the cement generated should be at least comparable to the physical and chemical properties of the “normal” cement; and b) the “new” cement should not cause any additional

environmental problems (in other words, one environmental problem should not be replaced by another). The potential risks should be minor compared to the ecological benefit obtained by recycling the waste.

Until now the RG generated in the TiO<sub>2</sub> industry has not found any use and has been disposed of in an authorized area. This policy has been costly, and for that reason the company decided to re-evaluate its options with this waste. In this direction, the work presented in this manuscript analyzes the viability of using red gypsum in the cement industry by analysing if the use of this waste in different proportions modifies/improves in any way the properties of the cement generated. We have checked if the cements manufactured from this waste comply with the quality standards required by Spanish legislation (behaviour of the matrix formed, calorimetry, resistance, etc), and if they are similar or better in quality than commercial cement (CEM). Knowing that large amounts of natural gypsum are used in cement production as a set retardant, by adding it to the clinker in a proportion that ranges from 3 to 5% [18], we have analyzed the possibility of using red gypsum as a substitute for natural gypsum in the production of cement.

## 2. MATERIALS AND METHODS

### 2.1. Material

The samples of raw materials (ilmenite and slag), and waste (“red gypsum”) used in this study have been collected from a titanium dioxide production plant located at 12 km from the city of Huelva, in south-western Spain. Five sampling campaigns were organised during a period of one month with sampling taking place every six days, in order to analyse the possible temporal variability of the sample characteristics. The total number of samples was 15. After collection, samples were dried at 105°C until reaching constant weight before analysis, except the red gypsum samples that were dried at 45°C to avoid the loss of their hydration water.

As the objective of our work was to check the possibility of substituting natural gypsum for red gypsum as a set retardant in the manufacture of cement, mixtures of varying percentages of red gypsum were added to conventional clinker (see table 1). The properties of these mixtures were compared to those of commercial cement (CEM), which has the following characteristics: its resistance category is 52.5 N/mm<sup>2</sup>, and is composed of a mixture of clinker (97%) and natural gypsum (3%). The different raw materials used in the mixtures of clinker-red gypsum, as well as the commercial cement taken as reference, then underwent also a physicochemical characterization. Prior to this, all the raw samples used in the cement studies were dried at 50°C until reaching constant weight (at this low temperature red gypsum does not lose its hydration), while the percentage of organic matter in representative aliquots was determined by the loss on ignition method at 550°C.

**Table 1. Proportions of clinker and red gypsum used in the three cements formed for this study. The characteristics of the commercial cement taken as reference are also given**

Name	CEM I, 52.5 N/SR	Clinker	Red Gypsum
CEM	100	-	-
YA	-	97.5	2.5
YB	-	95	5
YC	-	90	10

## 2.2. Methods Used for Physicochemical Characterization

### 2.2.1. Mineralogy

The mineralogical studies were performed by applying the X-ray diffraction technique, and in particular, the disoriented dust method with a Bruker D8 Advance system. For these analyses, we used the  $k_{\alpha}$  radiation of Cu, excited by 50 mA of intensity and 40 kV of voltage.

The mineralogical quantification of the samples was performed using Bruker EVA software with internal standards, noting that this technique is only valid for analyzing crystalline compounds.

### 2.2.2. Chemical analysis

The major elements were determined by applying the X-ray fluorescence (XRF) technique with a Philips PW-1004 X-ray system equipped with a tube of Sc-Mo and five different analyzer crystals. The spectra obtained were analyzed using super-Q manager software.

As this technique requires a maximum homogenization of the sample to be analyzed, the procedure was as follows: one gram of each dry sample and 10 grams of lithium tetraborate (material used for melting) were mixed with five drops of lithium iodide at 20%. Each mixture was then placed in a crucible of Pt-Au, and set in a special furnace to fuse the sample. The final result was homogeneous glass samples ready for measurement.

The inductively coupled plasma mass spectrometry (ICP-MS) technique was used to determine the trace elements. The determinations were achieved following the total dissolution of the samples, and their later dilution for placement in the ICP-MS system as 2% nitric acid solutions.

### 2.2.3. Granulometry

The granulometric analyses have been performed by using a Sympatec diffractometer that operates in a range between 0.90 and 175  $\mu\text{m}$ . This technique is based on the incidence of a monochromatic laser beam through a non-reactive liquid carrying a suspension of the sample to be analyzed. To provoke the total dispersion of the samples in the non-reactive liquid, isopropyl alcohol was used to remove the electronic and Van der Waals forces between the particles.

#### **2.2.4. Scanning electron microscopy (SEM) with X-ray microanalysis (XRMA)**

Microscopic information was obtained by using an automated scanning electron microscopy system (JEOL JSM-5410) working at 20 KV and equipped with an energy dispersive X-Ray (EDX) spectrometer. Aliquots of each sample were laid on conducting carbon tape and mounted on an aluminum frame for this purpose. In addition, by focusing on small spots of the samples, and by analyzing the X-ray fluorescence signals (generated by the impinging electrons) associated to these spots with the EDX system, the X-ray lines were identified and the elemental surface composition of each spot was obtained.

#### **2.2.5. Calorimetry**

To perform these analyses, a calorimeter of isothermic conduction (model THERMOMETRIC 3116/3239 TAM) was used. All the analyses were performed at a temperature of  $25.0 \pm 0.5$  °C, taking distilled water as a reference system, with five grams of the sample for analysis added to the calorimeter.

#### **2.2.6. Gamma spectrometry**

Gamma measurements were carried out using an XtRa coaxial Ge detector (Canberra), with 38% relative efficiency and FWHM of 0.95 keV at the 122 keV line of  $^{57}\text{Co}$  and 1.9 keV at the 1333 keV line of  $^{60}\text{Co}$ . The detector was coupled to a conventional electronic chain, including a multichannel analyser and was shielded with Fe 15 cm thick.

#### **2.2.7. Alpha spectrometry**

Th and U isotopes activity concentrations were determined in the samples by alpha-particle spectrometry. For the determination of these isotopes by alpha-particle spectrometry in the samples, a sequential well-established radiochemical method to the samples was applied [19]. In this method, the isotopes are electrodeposited onto stainless steel discs after its isolation from the bulk matrixes. The planchets were measured using an EG&G Ortec alpha spectrometry system with ion-implanted silicon detectors. Counting times ranged from 2 days to 4 days, depending on the activity concentrations and the recovery obtained in the chemical separation.

## **3. RESULTS AND DISCUSSION**

### **3.1. Physicochemical and Radiological Characterization of the Materials**

In Table 2, we can see that ilmenite is a NORM mineral due to its enrichment in natural radionuclides from the Th and U series, with a total concentration of some 500 Bq/kg for  $^{238}\text{U}$  and  $^{232}\text{Th}$ . On the opposite, the figures for slag are lower than those found in typical undisturbed soil (20-30 Bq/kg) [20]. The Clinker activity concentrations are around 20 Bq/kg for U and Th series, and present a value of 338 Bq/kg for  $^{40}\text{K}$ , being those similar to the unperturbed soils ones.

**Table 2. Average concentrations of dry Bq/kg activity of natural radionuclides in the raw material (ILM, SLAG, CLINK) and RG. Relative Humidity R.H (%). N.D. Under Detection.**

	R.H.	<sup>238</sup> U	<sup>226</sup> Ra	<sup>232</sup> Th	<sup>228</sup> Ra	<sup>40</sup> K
ILM	4.0	95 ± 10	110 ± 10	420 ± 15	440 ± 30	30 ± 5
SLAG	3.1	5.9 ± 0.6	6.1 ± 0.6	14 ± 1	9.0 ± 0.4	N.D
CLINK	3.8	21 ± 2	19 ± 1	16 ± 1	17 ± 1	338 ± 20
RG	46.3	20 ± 1	14 ± 1	127 ± 3	91 ± 3	12 ± 2

The radioactive content for RG is moderate, indicating that a minority fraction of the content in the treated raw material is accumulated in this co-product, for example 127 Bq/kg <sup>232</sup>Th and 91 Bq/kg for <sup>228</sup>Ra. No radiological concern then appears associated to the potential use of RG in cement.

In relation to the majority metals, table 3, ilmenite has the following composition: Fe<sub>2</sub>O<sub>3</sub> (44 %) and TiO<sub>2</sub> (~ 50 %), with low percentages of SiO<sub>2</sub> (0.7 %), MnO (1.3 %) and MgO (0.33 %), [12]. In contrast, the slag is much richer in titanium than the ilmenite (75 % TiO<sub>2</sub>), as expected, but poorer in iron (~ 11 % Fe<sub>2</sub>O<sub>3</sub>) [13]. On the other hand, the majority composition of RG is: 27 % SO<sub>3</sub> and 33 % of CaO as expected, but with a significant iron hydroxide content (14 %) which gives it its characteristic dark red colour [21-22]. Also surprising is the high titanium content in the RG (~ 7 % TiO<sub>2</sub>). The percentages of CaO and SO<sub>3</sub> in the red gypsum are similar to those normally found in natural gypsum or in analogues of natural gypsum such as phosphogypsum [23], while the results from the clinker and cement in our experiments clearly lie within the range of values found in the literature for these compounds.

**Table 3. Concentration of majority elements (expressed as oxides in %) in Ilmenite, slag, red gypsum and conventional clinker. Concentrations in the commercial cement taken as reference is also shown, as well as the range of concentrations normally found in the analysis of clinkers (data from the literature [24-25])**

	ILM	SLAG	RG	CLINK	CEM	Portland clinker
L.O.I.	-	-	21.1	0.85	2.54	
SiO <sub>2</sub>	0.71	2.5	1.2	22	20	19-23
Al <sub>2</sub> O <sub>3</sub>	0.71	2.3	1.4	5.3	6.2	3.5 -6.5
CaO	0.05	0.56	33	66	62	62-68
Fe <sub>2</sub> O <sub>3</sub>	44	11	14	2.8	2.3	0.5 – 6.0
MgO	0.33	5.1	1.4	1.4	-	0.5 – 4.0
MnO	1.3	0.26	0.35	-	0.18	-
TiO <sub>2</sub>	50	75	7.6	-	-	-
SO <sub>3</sub>	<0.01	0.18	27	0.53	2.8	2.0 – 3.5
Na <sub>2</sub> O	<0.01	<0.01	0.12	0.04	0.27	0.3 – 1.2
K <sub>2</sub> O	<0.01	<0.01	<0.01	1.0	0.73	-



One fact regarding red gypsum that needs to be mentioned is its LOI. Spanish law stipulates a maximum for this magnitude in commercial cements, which should be always lower than 5 %. Taking in consideration the LOI of the red gypsum and clinker analyzed in this study, and assuming an addition of 10 % of red gypsum at most to the clinker to form the cement, the resulting LOI of the mixture, at around 3 %, would clearly be below the legal maximum.

The diffractogram obtained for RG, figure 2, indicated as expected, that the main crystalline phase is  $\text{CaSO}_4 \cdot 2\text{H}_2\text{O}$ , being it very similar to that found in the literature for natural gypsum [23], giving greater confidence in the use of red gypsum as a substitute for natural gypsum in cement.

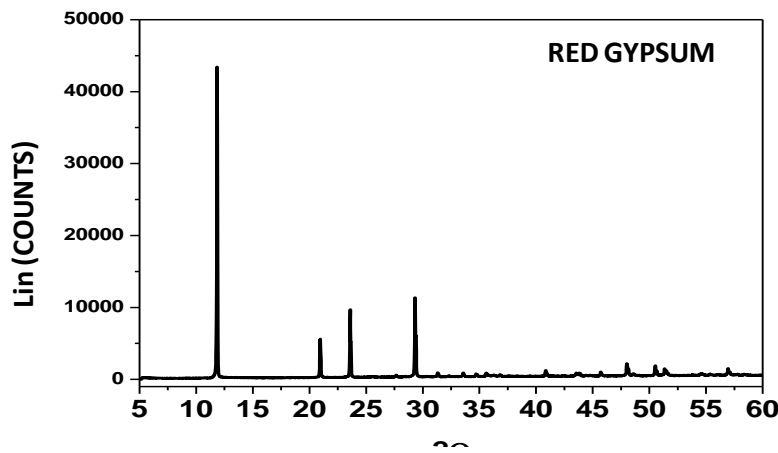


Figure 2. Diffractogram obtained for the RG sample

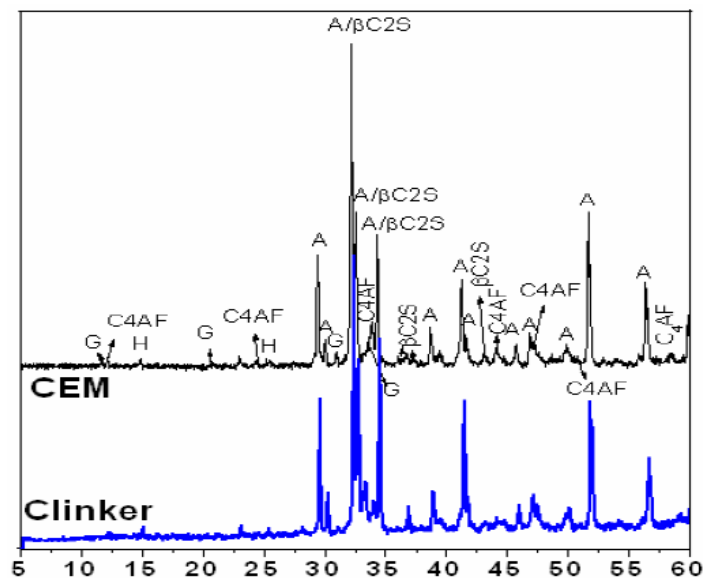


Figure 3. Diffractograms obtained for the conventional clinker used in this work, and for the commercial cement (CEM) taken as reference. (Symbols: A ( $\text{C}_3\text{S}$ = allite) ;  $\beta$  ( $\text{C}_2\text{S}$ = bellite) ;  $\text{C}_4\text{AF}$  (ferritic phase);  $\text{C}_3\text{A}$  (tricalcium aluminate), and G (gypsum))

On the other hand, in Figure 3 it is shown the diffractograms obtained in the analysis of a) the commercial cement taken as reference and, b) the clinker used in the mixtures formed with red gypsum.

These diffractograms are concordant with the found ones in the literature for the same materials [24], and have a special feature: both diffractograms are quite similar but with one essential difference: a peak in the gypsum phase appears in the cement diffractogram but, obviously, does not appear in the clinker diffractogram. We insist once again that the role of gypsum in the cement is to act as a set retardant in its solidification.

Both the commercial cement and the raw clinker are formed by a mixture of crystalline phases, the majority compounds being: allite ( $C_3S$ ) [ $3(\text{CaO})\cdot\text{SiO}_2$ ] and bellite ( $C_2S$ ) [ $2(\text{CaO})\cdot\text{SiO}_2$ ]. In addition, they have minority phases such as the tricalcium aluminate ( $C_3A$ ) [ $3(\text{CaO})\cdot\text{Al}_2\text{O}_3$ ] and ferritic phases ( $C_4AF$ ) [ $4(\text{CaO})\cdot\text{Al}_2\text{O}_3\cdot\text{Fe}_2\text{O}_3$ ]. Table 4 compiles the percentages for the main mineral compounds found in the commercial cement analyzed in this work. The table also includes the ranges of the same mineral phases in similar cements in the literature, being possible to see how the results from the commercial cement examined in our study fall within the ranges expected.

As a final step, the three mixtures of clinker-red gypsum generated by using different percentages of red gypsum (see Table 1) were also analyzed. The mineralogical characterizations for the three mixtures were performed 28 days after production, with the resulting diffractograms presented in Figure 4. By comparing these spectra to those obtained for the raw materials (see Figure 3), it is possible to conclude that, as a consequence of the hydration reactions in the cement, the peaks associated to the presence of allite diminish in intensity while new peaks appear which are linked to the formation of new compounds: portlandite and ettringite.

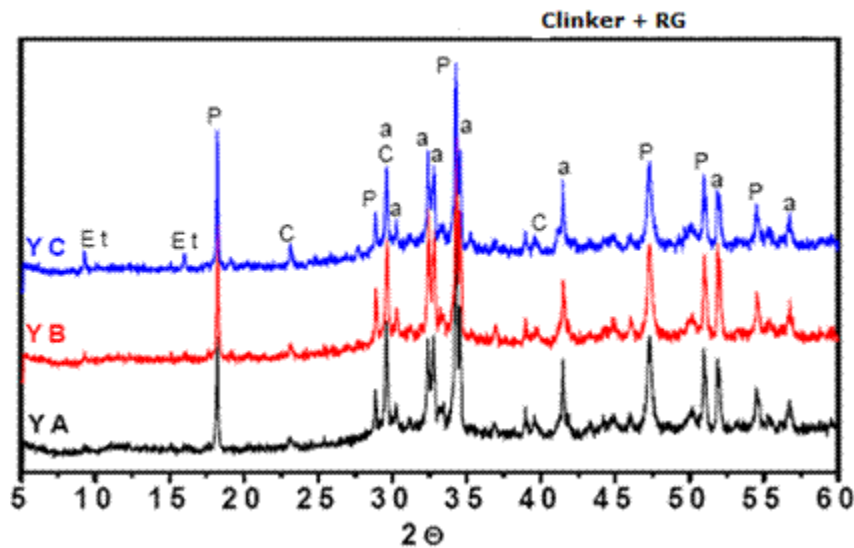


Figure 4. Diffractograms obtained for the three cements generated with red gypsum as an additive (see Table 1). (Symbols: A = allite; P = portlandite; Et = Ettringite; C= calcite)

**Table 4. Concentrations (in %) of the main mineralogical phases found in the commercial cement (CEM) taken as reference in this work. Also shown are the ranges of concentrations for the same mineral phases found in the literature for cements.**

Phase	Commercial cement (CEM)	Literature data for cements
Allite	57.1	42 – 67
Bellite	14.5	9 – 30
Tricalcium Aluminate	12.6	6 – 14
Ferrite	6.9	1 – 12

The presence of ettringite is only clearly detected in the YC sample, i.e., in the sample with the biggest percentage of red gypsum (10%). It was not observed in the two other mixtures due to the low percentage of red gypsum added. The ettringite is formed as a consequence of the complete reaction of the gypsum in the tricalcium aluminate phase, and is a good indication that red gypsum added to clinker reacts in a similar way to conventional gypsum.

In order to analyze how the red gypsum impurities are incorporated in the final cement product, a detailed study by SEM was made of the YC cement sample. This sample is the one that contains the biggest proportion of red gypsum (10%). The SEM analyses were performed in the BSE mode, i.e., by analyzing the image generated, after impinging the electron beam on the sample, by means of backscattered electrons. In this SEM/BSE mode, and knowing that the probability of backscattering increases with the Z of the material impinged on by the electron beam, it is possible to obtain an image where the contrast between the several brightness is an indication of the presence of elements with a different Z (the bright areas in the image correspond to elements with a higher Z than to the elements in the darker areas). In this sense, it is necessary to point out that all the main elements in the clinker and the red gypsum are characterized by a low Z, and that only the presence of titanium and iron impurities corresponds to elements with a higher Z.

A typical SEM image obtained with the YC sample is shown in Figure 5. This image enables us to reconfirm that the red gypsum has reacted completely with the mineral phases of the clinker because no particles of calcium sulphate were detected. In Figure 5, it is possible to observe a main dark matrix (point 2) corresponding to the cement formed, with a composition typical of a C-S-H (Calcium Silicate Hydrate) gel, Ca-Si ratio =  $2.2 \pm 0.1$ . The bright particles imbedded in the matrix are formed either by iron (point 1) or by iron plus titanium (point 3), as can be deduced from the corresponding X-ray spectra obtained by XRMA at these points, which are also shown in Figure 5.

All the SEM-XRMA results indicate that the red gypsum added to the clinker reacts in a similar way to the natural gypsum, with all the particles enriched in iron and titanium trapped in the main matrix. This is extremely important because it greatly reduces the potential leaching of the iron and titanium contaminants in the cement formed and, consequently, limits their potential harm to the environment.

In addition, one very important aspect to take into account in cement making is the grain size of the different materials used in its formation. Figure 6 shows the granulometry of the clinker and the red gypsum used in the mixtures formulated for analysis in this work.

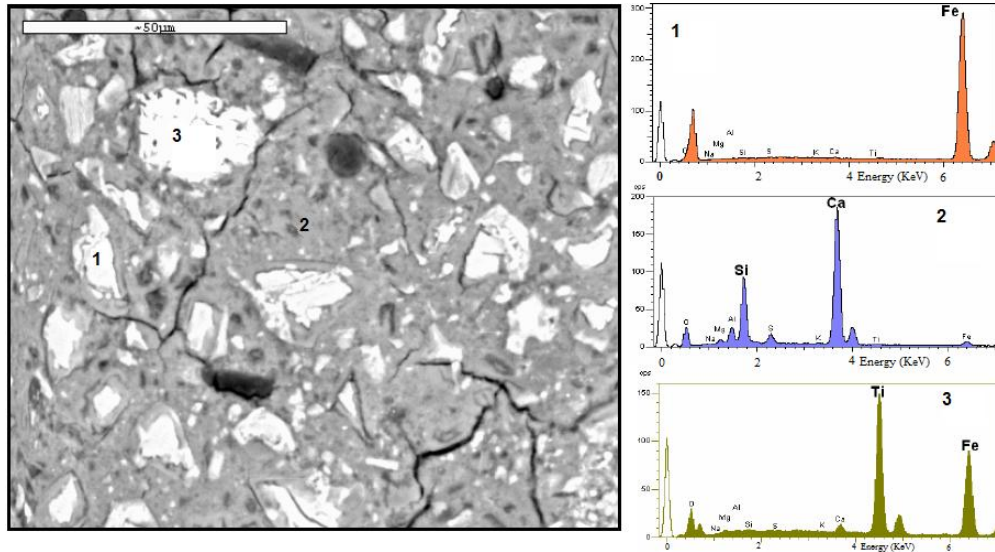


Figure 5. SEM image, obtained in the BSE mode (left-side image) of the cement formed through the mixture of conventional clinker with 10% of red gypsum (YC sample, Table 1). The X-ray spectra corresponding to some spots in the sample are also shown (right-side images).

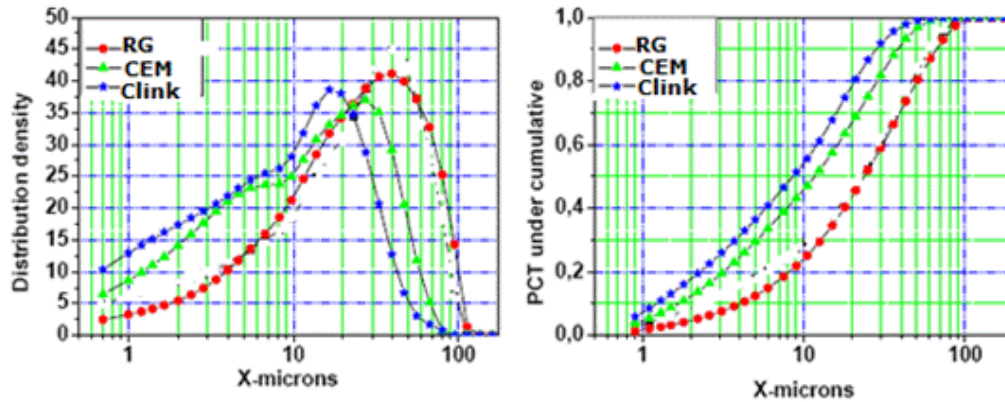


Figure 6. Granulometric distribution determined in the conventional clinker (Clink) and in the red gypsum (RG) used as raw materials in this work. Also, for comparison, the granulometric distribution determined in the commercial cement (CEM) taken as reference is shown.

The granulometry of the reference commercial cement is also included for comparison. The data obtained shows that red gypsum has a maximum granulometric distribution of around 40  $\mu\text{m}$ . This is slighter higher than the commercial cement maximum (about 30  $\mu\text{m}$ ) and double that of clinker (about 20  $\mu\text{m}$ ), which indicates that red gypsum is an appropriate additive as a retardant in cement solidification

### 3.2. Test Analyses to Evaluate the Viability of the Cements Formed by Adding Red Gypsum

The first step after the formation of the three dried mixtures of clinker with red gypsum (see Table 1) was to determine the appropriate water/cement (W/C) relation in weight terms for obtaining a “normal” consistency of the paste formed, as defined in the UNE- EN 196-3 regulation in the Spanish law. A normalized Vicat apparatus with a rod 50 mm in length and 10 mm in diameter was used for this purpose, and various moulds of the three mixtures were fabricated with different W/C proportions. All the moulds were 40 mm in height, with a shape of a truncated cone with lower and upper diameters of 70 and 80 mm, respectively. For each mixture, the optimum W/C ratio corresponded to the penetration of the rod in the mould to a depth of 34 mm.

The optimum W/C ratios for the three different cements formed with red gypsum are shown in table 5. This table also presents the optimum W/C ratio obtained for the commercial cement used as reference. All the W/C ratios are quite similar, with no significant differences found between the commercial and red gypsum cements.

#### 3.2.1. Setting times of the cements formed

The setting times of the three cements formed by using different proportions of red gypsum as an additive were also obtained with a Vicat apparatus, equipped in this instance with a normalized noodle with a 1.13 mm diameter. All the cements were analyzed as pastes formed with the previously determined optimum W/C ratios. The national protocol for achieving setting times is UNE-EN 196-3, which is based on the study of the depth of penetration of the noodle in the mould at different positions. At time zero, the noodle penetrates until the base of the mould. When the noodle has penetrated to a depth of 4 mm above the base, the hardening of the cement is considered to have started (initial setting time). When the noodle has penetrated only 0.5 mm into the mould, the cement hardening is deemed to have finished (final setting time).

The hardening of cement can be defined as the change over time that is produced in the consistency of the paste formed until it acquires the consistency of a solid. Table 5 compiles the setting times determined in our laboratory for the three red gypsum cements under analysis, and also those for the commercial cement taken as reference. The setting times for the three red gypsum cements are comparable to those obtained for the commercial cement.

**Table 5. Setting times determined following a normalized protocol for the various cements formed by using different proportions of red gypsum. For comparison, the setting times determined for the commercial cement taken as reference in this work are shown**

Sample	Optimum W/C	Initial setting time (min)	Final setting time (min)
(CEM) Commercial cement	0.27	139	224
YA (2.5% RG)	0.29	82	129
YB (5% RG)	0.27	108	298
YC (10% RG)	0.29	216	351

**Table 6. Minimum and maximum setting times permitted for cements of different resistance, according to Spanish legislation**

Cement resistance class	Setting times	
	Initial (min)	Final (min)
32.5 N	≥ 75	≤ 720
32.5 R		
42.5 N	≥ 60	
42.5 R		
52.5 N	≥ 45	
52.5 R		

In order to see if the setting times for the red gypsum cements fulfill the requirements established in Spanish law (regulation UNE-EN 196-3), table 6 shows the minimum and maximum values stipulated for the setting times of cements with different resistances.

The data show that the addition of red gypsum in the proportions used in this work leads to setting times that are within those required by national legislation, and it is noteworthy that the initial and final setting times are prolonged by increasing the proportion of red gypsum used as an additive in cement fabrication, further underlining the role of red gypsum as a retardant in the hardening of cement. Adding higher percentages of red gypsum extends the initial and final setting times. For the YC cement (10% red gypsum) these increases are of 55.4% (from 139 to 216 min) and 56.7% (from 224 to 351 min) in the initial and final setting times, respectively, in relation to the commercial cement.

### 3.2.2. Volumetric stability tests

In order to analyze the possible risks of short-time expansion, which can affect the red gypsum cements formed, the Le Chatelier test was performed following the UNE-EN 196-3 regulation. This test is based on the use of a small cylindrical mould opened by a generatrix and closed with two noodles with a fixed distance between them. The moulds are filled with the paste of the cement to be analyzed (the paste was formed at the optimum W/C ratio determined previously), stored in a humidity chamber for 24 hours and, finally, half of them are submerged in boiling water for 3 hours, and the other half in water at room temperature for 7 days. The increase in the distance between the ends of the two noodles gives a value that can be used as a reference of the expansion that the tested cement undergoes.

In Table 7, the reference expansion values for the three red gypsum cements, as well as for the commercial cement, are shown. The results show that the presence of red gypsum in the cements formed does not cause any significant modification in its expansion behavior in comparison to the commercial cement, irrespective of the proportion of red gypsum used as an additive. And more important, the values comply with Spanish legislation, which indicates that the reference value for expansion obtained through the le Chatelier test for any cement should be lower than 10 mm

### 3.2.3. Mechanical resistance tests

Mortars (sand and cement mixed in a proportion of 3:1) were used to develop tests to evaluate the compressive and flexural strength of the cements formed with red gypsum. These

mortars were made from sand with a SiO<sub>2</sub> content of about 99% in mass. The optimum W/C values in these mortars were determined strictly according to regulation UNE 83.811-92 in Spanish law.

Once the different mortars were formed, their binding and compressive resistances were measured in prismatic test samples (40 x 40 x 160 mm) two and 28 days after their formation. Flexural resistance was determined by applying the method of centered and concentrated loads to the prismatic samples, while the compressive tests were performed using the broken prismatic samples in the flexural tests, over surfaces of 40 x 40 mm.

The resistances to flexion and compression determined through these tests for the three red gypsum cements analyzed in this work are given in Table 9. Each result in this table is the average of three tests performed on three different samples formed from the same paste. The same table also shows the comparative results for the commercial cement (CEM).

**Table 7. Expansions (mm) determined in the volumetric stability tests applied to three cements formed with red gypsum and to the commercial cement taken as reference**

Commercial cement (CEM)						
	S. 1	S. 2	S. 3	S. 4	S. 5	S. 6
Initial measurement	17	17	15	16	16	16
after 24 hours	17	17	15	16	15	16
3 hours-100°C	15	15	16	-	-	-
7 days under water	-	-	-	17	15	16
Expansion (mm)	2	2	1	1	0	0
YA Sample (2.5% red gypsum)						
	S. 1	S. 2	S. 3	S. 4	S. 5	S. 6
Initial measurement	18	18	17	17	17	18
after 24 hours	20	21	19	20	19	21
3 hours-100°C	21	22	20	-	-	-
7 days under water	-	-	-	20	19	21
Expansion (mm)	1	1	1	0	0	0
YB Sample (5% red gypsum)						
	S. 1	S. 2	S. 3	S. 4	S. 5	S. 6
Initial measurement	18	18	16	18	18	17
after 24 hours	25	25	21	25	23	24
3 hours-100°C	25	26	22	-	-	-
7 days under water	-	-	-	25	23	24
Expansion (mm)	0	1	1	0	0	0
YC Sample (10% red gypsum)						
	S. 1	S. 2	S. 3	S. 4	S. 5	S. 6
Initial measurement	18	17	18	17	16	16
after 24 hours	23	22	23	20	21	20
3 hours-100°C	24	23	24	-	-	-
7 days under water	-	-	-	20	21	20
Expansion (mm)	1	1	1	0	0	0

**Table 9. Values of flexural and compressive resistances (MPa) determined in the three types of red gypsum cements analyzed in this work. For comparison, the results obtained with the same tests for the commercial cement (CEM) taken as reference are also shown**

Sample	W/C	Flexural strength		Compressive strength	
		2 days	28 days	2 days	28 days
Commercial cement (CEM)	0.40	6.8±0.33	10.1 ± 1.2	34.4 ± 0.4	61.3 ± 1.0
YA (2.5% red gypsum)	0.54	4.2±0.15	9.8 ± 0.6	17.8 ± 0.3	51.7 ± 0.6
YB (5% red gypsum)	0.52	5.4±0.25	8.2 ± 2.7	23.1 ± 0.3	57.9 ± 1.0
YC (10% red gypsum)	0.52	7.6±0.80	10.8 ± 0.8	31.5 ± 0.8	59.6 ± 1.5

**Table 10. Values of compressive strengths (MPa) according to UNE-EN 196-1. R High initial strengths and N normal strengths**

Cement resistance class	Initial strength		Final strength	
	2 days	7 days	28 days	
32.5 N	-	≥ 16.0	≥ 32.5	≤ 52.5
32.5 R	≥ 10	-		
42.5 N	≥ 10	-	≥ 42.5	≤ 62.5
42.5 R	≥ 20	-		
52.5 N	≥ 20	-	≥ 52.5	-
52.5 R	≥ 30	-		

The critical evaluation of the results in Table 9 leads to the following conclusion: it seems that the mechanical behaviour of the cements formed improves when more red gypsum is added to the cements, thereby approaching the resistance values of the commercial cement. In fact, in the YC sample (10 % red gypsum) the mechanical resistance values are similar to those for the commercial cement. This is important, as it supports the use of red gypsum as an additive in the formation of cements and because it is possible to reduce the amount of clinker used, with all the economic benefits that this entails (cost savings). In this sense, it is necessary to remember that the commercial cement taken as reference in our study is approximately 97% clinker and 3 % natural gypsum.

With low proportions of red gypsum, the mechanical resistance values obtained are slightly lower than those for the commercial cement. And as can be deduced from table 10, the mechanical resistance values for the three red gypsum cements analyzed comply with regulation UNE-EN 196-1.

#### **3.2.4. Physical retraction tests**

Mortar samples (under the same conditions and sand/cement proportions as for the mechanical tests) were made to determine the linear retraction in the red gypsum cements that occurs due to their progressive dryness. The mortars were tested in accordance with regulation ASTM C 596-89: “Standard Test Method for Drying Shrinkage of Mortar Containing Portland Cement”. Special moulds were filled with the mortar samples for this purpose, as described in this protocol.



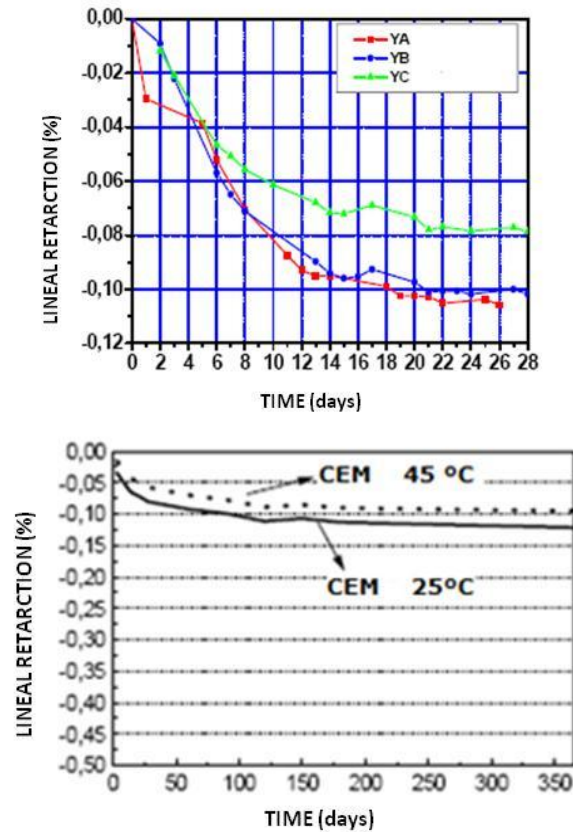


Figure 7. Linear retraction curves obtained for the three cements formed with red gypsum (left). For comparison, the linear retraction curves for the commercial cement at 25 °C y 45 °C are also shown (right)

The linear retraction values were determined in prismatic test samples (25.4 x 25.4 x 287 mm), and the results from the three red gypsum cements and the commercial cement are shown in Figure 7. Here we observe how the major retractions occur during the first days of reaction. Then as the cement hydration times progress, the linear retractions diminish until to be practically constant in the final days.

The results also show that the addition of red gypsum to the clinker improves the linear retraction of the cements formed in comparison to the commercial cement. As higher percentages of red gypsum are added to the cement, lower retractions are produced. All these linear retraction values are within the range permitted by Spanish legislation, further increasing confidence in the viability of red gypsum as a set retardant additive in the fabrication of cements.

### 3.2.5. Calorimetric studies

Calorimetric analyses of the three red gypsum cements were performed in order to determine the total heat liberated in their hydration processes, as well as the velocity of heat liberation. During hydration, transitions occur from states of high to low energy, being liberated the excess energy in the form of heat.

**Table 11. Determinations performed in the calorimetric analysis of the three red gypsum samples analyzed in this work. For comparison, the determinations performed in the clinker used for the fabrication of the red gypsum cements, and in the commercial cement (CEM) taken as reference, are also shown**

Sample	Peak of Acceleration-Deceleration			TOTAL HEAT AFTER 60 HOURS (kJ/kg)
	V(kJ/kg·h)	t <sub>v</sub> (h)	Q <sub>v</sub> (Kj/kg)	
Cement	17.60	6.40	86.4	254.3
Clinker	12.50	7.20	71.4	258.3
YA	15.89	9.09	39.4	253.3
YB	14.30	11.30	96.7	231.0
YC	12.56	9.95	84.0	269.2

Most commercial cements liberate 50 % of their heat during the first three days of hydration. In addition, if the curve plotted for typical cement represents the liberation of heat versus time, it is observed that a maximum peak of acceleration-deceleration appears after about six hours. This peak is associated to the formation and precipitation of the C-S-H gel, the main product generated in the hydration of the cements.

By applying the isothermic conduction calorimetry technique, we have determined the velocity of heat liberation, the time elapsed until the appearance of the acceleration peak, the total heat liberated associated to the peak, and the total heat liberated after 60 hours for the three red gypsum cements and the commercial cement analyzed in this work. The values obtained are compiled in Table 11.

These values clearly indicate that the addition of red gypsum diminishes the velocity of heat liberation in the acceleration-deceleration peak, down to 12.6 kJ/kg.h in the YC sample, which is 28 % lower than that obtained for the commercial cement. The addition of red gypsum also retards the appearance of this peak until 9.95 h in the YC sample or 11.2 h in the YB sample. On other hand, the total heat liberated in the cements formed with red gypsum is fairly similar to that in the commercial cement, and is even slightly higher in the YC sample, but lower in the YB sample, 231.0 kJ/kg. The addition of red gypsum delays the reaction and formation of the C-S-H gel, which in energy terms is produced in a very similar way to the commercial cements.

### **3.2.6 Environmental impact evaluation**

We have finally assessed the environmental impact of the use of red gypsum in cement manufacturing. Table 12 shows the critical concentration values that define the ecotoxicity threshold, i.e, if the concentration of a metal is lower than this limit, it does not generate significant environmental impact [26].

As observed in this table, red gypsum metal concentrations are lower than the ecotoxicity limits. Only Cr concentration is slightly higher than this threshold, but given that the maximum amount of red gypsum in cement is about 10%, the Cr concentration in the final cement will be well below this limit. So, it is possible to affirm that the addition of red gypsum to the manufacturing of cement is not a threat to the environment.

**Table 12. Comparison of critical concentration values [26] and RG**

Element	Critical concentration (mg/kg)	RG (mg/kg)	Soil (*) (mg/kg)
As	20-50	10	4.8
Cd	3-8	1	0.09
Co	25-50	16	17
Cr	75-100	109	92
Ni	100	30	47
Pb	100-400	19	17
Zn	70-400	212	67

(\*) Continental Crust composition [27].

## CONCLUSIONS AND FINAL REMARKS

After a detailed physicochemical characterization of the raw materials and cements considered in this study, and the performance of an ample set of physico-mechanical and chemical tests, the main conclusions regarding to the possible use of red gypsum in the fabrication of cements and mortars are the following:

- a) Red gypsum retards the setting times of the cements, in a similar way to natural gypsum. The addition of red gypsum also reduces the linear retraction of the fabricated cements.
- b) With red gypsum as an additive, the cements offers mechanical resistances equivalent to those ones obtained with natural gypsum.
- c) From the mineralogical and microstructural point of view, red gypsum produces the same mineral phases as natural gypsum. In addition, the grain size distribution of red gypsum is optimal for mixing with clinker as a substitute for natural gypsum.
- d) The particles of Fe and Ti present as contaminants in red gypsum are physically fixed in the cement matrixes formed, and do not constitute a potential source of contamination via leaching into the environment.

These conclusions enable us to conclude that red gypsum can be safely applied as a substitute for natural gypsum in the fabrication of commercial cements without decreasing the quality of the cements generated, and without causing any environmental impact. A proportion of red gypsum as high as 10 % can be used in the manufacture of cements and still complies with all the quality requirements in Spanish legislation.

## REFERENCES

- [1] Kacimi, L., Simon-Masseron, A., Ghomari, A. & Derriche, Z. (2006). Reduction of clinkerization temperature by using phosphogypsum. *Journal of Hazardous Material* B137, 129-137.

- 
- [2] Kuryatnyk, T., Angulski Da Luz, C., Ambroise, J. & Pera, J. (2008), Valorization of phosphogypsum as hydraulic binder. *Journal of Hazardous Material*, 160, 681-687.
- [3] De Michelis, Ida, Ferella, F., Beolchini, F., Olivieri, A. & Veglió, F. (2008). Characterisation and classification of solid wastes coming from reductive acid leaching of low grade manganiferous ore. *Journal of Hazardous Material*, doi: 10.1016/j.jhazmat., 06.024.
- [4] Liu Yong, Lin Chuxia, Wu Yonggui. (2007). Characterization of red mud derived of from a combined Bayer Process and bauxite calcination method. *Journal of Hazardous Material*, 146, 255-261.
- [5] Deydier Erich, Guilet Richard, Sarda Stéphanie, Sharrock Patrick. Physycal and chemical characterization of crude meat and bone meal combustion residue: "waste or raw material?". *Journal of Hazardous Materials B121* (2005) 141-148.
- [6] Shen, W., Zhou, M., Ma, W., Hu, J. & Cai, Z. (2007). Investigation on the Application of Steel Slag-Fly Ash-Phosphogypsum Solidified Material as Road Base Material, *Journal of Hazardous Materials*, doi:10.1016/j.jhazmat.2008.07.125
- [7] Potgieter, J. H., Horne, K. A, Potgieter, S. S. & Wirth, W. (2002). An evaluation of the incorporation of a titanium dioxide producer's waste material in Portland cement clinker. *Materials Letters*, 57, 157-163.
- [8] Chen, G., Lee, H., Young, K. L., Yue, P. L., Wong, A., Tao, T. & Choi, K. K. (2002). Glass recycling in cement production: and innovative approach. *Waste Management*, 22, 747-753
- [9] Tsakiridis, P. E., Agatzini-Leonardou, S. & Oustadakis, P. (2004). Red mud addition in the raw meal for the production of portland cement clinker. *Journal of Hazardous Material*, 116, 103-110
- [10] Shih, P. H., Chang, J. E., Lu, H. C. H. & Chiang, L. C. H. (2005). Reuse of heavy metal-containing sludges in cement production. *Cement Concrete Research*, 35, 2110-2115.
- [11] Alp, I., Deveci, H., Yazici, E. Y., Türk, T. & Süngün, Y. H. (2009). Potential use of pyrite cinders as raw material in cement production: Results of industrial scale trial operations. *Journal of Hazardous Material*, 166, 144-149
- [12] Chernet, T. (1999). Applied mineralogical studies on Australian sand ilmenite concentrate with special reference to its behavior in the sulphate process. *Minerals Engineering*, Vol 12. No 5, 485-495.
- [13] Pistorius, P. C. & Coetzee, C. (2003). Physicochemical aspects of titanium slag production and solidification. *Metall. Mater. Trans.*, B 34B, 581-588.
- [14] Pesl, J. & Eric, R. H. (2002). High temperature carbothermic reduction of  $\text{Fe}_2\text{O}_3\text{-TiO}_2\text{-MxOy}$  oxide mixtures. *Miner. Eng.*, 15, 971-984.
- [15] Sahoo, P. K., Galgali, R. K., Singh, S. K., Bhattacharyee, S., Mishra, P. K. & Mahanty, B. C. (1999). Preparation of titania-Rich Slag by plasma smelting of ilmenite. *Scand. J. Metal.*, 28, 243-248.
- [16] Pourabdoli, M., Raygan, S. h., Abdizadeh, H. & Hanaei, K. (2006). Production of high titania slag by Electro-Slag Crucible Melting (ECSM) process. *International journal of Mineral Processing*, 78, 175-181
- [17] Zelikman, A. N., Kerin, O. E. & Samsonov, G. V. (1966). Metallurgy of Rare Metals. Israel Program for Scientific Translation Ltd., *Jerusalem*, 155-212.

- [18] Potgieter, J. H., Potgieter, S. S. & Mccrindle, R. I. (2004). A comparison of the performance of various synthetic gypsums in plant trials during the manufacturing of OPC clinker. *Cement Concrete Research*, 34, 2245–2250.
- [19] Holm, E. & Fukai, R. (1977). Method for multi-element alpha spectrometry of actinides and its application to environmental radioactivity studies. *Talanta*, 24, 659-64.
- [20] United Nations Scientific Committee On The Effects Of Atomic Radiation (Unsear) (2000). Report of the United Nations Scientific Committee on the Effects of Atomic Radiation, United Nations, New York.
- [21] Fauziah, I., Zaayah, S. & Jamal, T. (1996). Characterization and land application of red gypsum: a waste product from the titanium dioxide industry. *The Science of the Total Environment*, 188, 243-251.
- [22] Gázquez, M. J., Bolívar, J. P, Garcia-Tenorio, R. & Vaca, F. (2009). Physicochemical characterization of raw materials and co-products from the titanium dioxide industry. *Journal of Hazardous Material*, 166, 1429-1440.
- [23] Chandara Chea, Azizi Khairun, Azizl Mohd, Ahmad Zainal Arifin, Sakai Etsuo, (2009). Use of waste gypsum to replace natural gypsum as set retarders in portland cement. *Waste Management*, 29, 1675-1679.
- [24] Hewlett, P. C. (1998). Chemistry of cement and concrete. Four edition, Elsevier Butterworth- Heinemann editorial, Oxford.
- [25] Vangelatos I., Angelopoulos, G. N. & Boufournos, D. (2009). Utilization of ferroalumina as raw material in the production of Ordinary Portland Cement. *Journal of Hazardous Material*, 168, 473-478.
- [26] Kabata-Pendias, A. & Pendias, H. (2001). Trace elements in soils and plants. CRC Press., 413.
- [27] Gao, R. (2003). Composition of the Continental Crust, Treatise of Geochemistry, vol. 3, Elsevier, the Crust, pp. 1–64.